Rsd balances (p)ppGpp level by stimulating the hydrolase activity of SpoT during carbon source downshift in *Escherichia coli*

Jae-Woo Lee[a,1], Young-Ha Park[b,1], and Yeong-Jae Seok[a,b,2]

[a]Department of Biophysics and Chemical Biology, Seoul National University, Seoul 08826, Republic of Korea; and [b]School of Biological Sciences and Institute of Microbiology, Seoul National University, Seoul 08826, Republic of Korea

Edited by Alan D. Grossman, Massachusetts Institute of Technology, Cambridge, MA, and approved May 22, 2018 (received for review December 27, 2017)

Bacteria respond to nutritional stresses by changing the cellular concentration of the alarmone (p)ppGpp. This control mechanism, called the stringent response, depends on two enzymes, the (p)ppGpp synthetase RelA and the bifunctional (p)ppGpp synthetase/hydrolase SpoT in *Escherichia coli* and related bacteria. Because SpoT is the only enzyme responsible for (p)ppGpp hydrolysis in these bacteria, SpoT activity needs to be tightly regulated to prevent the uncontrolled accumulation of (p)ppGpp, which is lethal. To date, however, no such regulation of SpoT (p)ppGpp hydrolase activity has been documented in *E. coli*. In this study, we show that Rsd directly interacts with SpoT and stimulates its (p)ppGpp hydrolase activity. Dephosphorylated HPr, but not phosphorylated HPr, of the phosphoenolpyruvate-dependent sugar phosphotransferase system could antagonize the stimulatory effect of Rsd on SpoT (p)ppGpp hydrolase activity. Thus, we suggest that Rsd is a carbon source-dependent regulator of the stringent response in *E. coli*.

carbon source downshift | phosphotransferase system | protein–protein interaction | stringent response | TGS domain of SpoT

Bacteria possess several molecular mechanisms that allow them to respond and adapt to various environmental stresses. The stringent response is a stress response of bacteria (and plant chloroplasts), which orchestrates pleiotropic adaptations to nutritional starvation and some other stress conditions by fine-tuning the cellular levels of the "alarmones" ppGpp and pppGpp [collectively named (p)ppGpp] (1, 2). As the effector molecule of the stringent response, (p)ppGpp regulates a variety of biological processes, such as growth, adaptation, secondary metabolism, survival, persistence, cell division, motility, biofilms, development, competence, and virulence (2). In *Escherichia coli*, the intracellular level of (p)ppGpp is regulated by two enzymes, RelA and SpoT. RelA catalyzes the pyrophosphorylation of GDP (or GTP) using ATP to synthesize (p)ppGpp in a ribosome-dependent manner (3). The bifunctional enzyme SpoT has a strong (p)ppGpp hydrolase activity, converting (p)ppGpp into GDP (or GTP) and pyrophosphate (PPi), and a weak (p)ppGpp synthetase activity (4, 5). During amino acid starvation, ribosomes containing uncharged tRNAs accumulate, thereby activating the (p)ppGpp synthetase activity of RelA (6). SpoT responds to various nutrient stresses, such as carbon (7), iron (8), phosphate (9), and fatty acid starvation (10) with its (p)ppGpp synthetic and hydrolytic activities to balance cellular (p)ppGpp concentrations.

(p)ppGpp coordinates the transcriptome and metabolism in response to many sources of nutrient stress to facilitate bacterial adaptation (2). Regulation of transcription by (p)ppGpp has been demonstrated in a genome-wide scale in many bacterial species. (p)ppGpp, in conjunction with DksA, directly binds to RNA polymerase to inhibit transcription from rRNA and tRNA promoters (11), whereas they activate transcription from amino acid biosynthesis promoters and some other σ^{70} promoters in *E. coli* (12). (p)ppGpp also directly binds and inhibits translational GTPases (IF2, EF-G, and EF-Tu), DNA primase (DnaG), polyphosphate kinase (PPK), and lysine decarboxylase LdcI, whereas its direct binding to RelA activates (p)ppGpp synthesis (13). In Gram-positive bacteria, (p)ppGpp binds and inhibits enzymes required for the GTP synthesis pathway and negatively impacts transcription and ribosome assembly rather than by directly binding to RNA polymerase (14, 15).

Maintaining proper intracellular (p)ppGpp levels is important in cell physiology. To adjust appropriate intracellular (p)ppGpp levels in response to nutrient starvation, the (p)ppGpp hydrolase activity of SpoT plays a pivotal role because it is the only enzyme capable of hydrolyzing (p)ppGpp in *E. coli*. Therefore, the *spoT*-null mutant exhibits uncontrolled accumulation of (p)ppGpp, which leads to the severe inhibition of cell growth (7). However, little is known about how the (p)ppGpp hydrolase activity of SpoT is regulated except for its inhibition by accumulated uncharged tRNA (5). Thus, we assumed the existence of a molecular mechanism stimulating the reaction of SpoT-catalyzed (p)ppGpp hydrolysis.

In a recent study, it was found that dephosphorylated HPr of the bacterial phosphoenolpyruvate:sugar phosphotransferase system (PTS) interacts with and antagonizes the anti-σ activity of Rsd (16), which was named for its regulatory effect on the σ factor RpoD (σ^{70}) (17). The PTS catalyzes the phosphorylation-coupled transport of various sugars. This system consists of two general components, enzyme I (EI) and the histidine-containing phosphocarrier protein HPr, which are common to most PTS

Significance

Most bacteria accumulate the molecular alarmone (p)ppGpp to divert resources away from growth and division toward biosynthesis under various nutrient limitations. Despite its crucial role, uncontrolled accumulation of this alarmone causes severe growth inhibition and cell death. Thus, fine-tuning the cellular (p)ppGpp level is required to ensure survival and adaptation under harsh nutritional conditions. Here, we identify Rsd as a stimulator of the (p)ppGpp-degrading activity of SpoT during carbon source downshift in *Escherichia coli*, and this regulation is controlled by the phosphorylation state of HPr, a general component of the PEP-dependent sugar transport system. This study establishes a direct link between sugar signaling and the bacterial stringent response.

Author contributions: J.-W.L., Y.-H.P., and Y.-J.S. designed research; J.-W.L. performed research; Y.-H.P. contributed new reagents/analytic tools; J.-W.L., Y.-H.P., and Y.-J.S. analyzed data; and J.-W.L., Y.-H.P., and Y.-J.S. wrote the paper.

The authors declare no conflict of interest.

This article is a PNAS Direct Submission.

See Commentary on page 7454.

[1]J.-W.L. and Y.-H.P. contributed equally to this work.

[2]To whom correspondence should be addressed. Email: yjseok@snu.ac.kr.

This article contains supporting information online at www.pnas.org/lookup/suppl/doi:10.1073/pnas.1722514115/-/DCSupplemental.

Published online June 18, 2018.

sugars, and several sugar-specific enzyme IIs (EIIs) (18, 19). Each EII complex generally consists of one integral membrane domain forming the sugar translocation channel (EIIC) and two cytosolic domains (EIIA and EIIB). EI transfers a phosphoryl group from PEP to HPr. HPr then transfers the phosphoryl group to EIIA, which phosphorylates EIIB. In the presence of a PTS sugar, the phosphoryl group of EIIB is transferred to the sugar that is transported through the EIIC channel across the membrane. Thus, the phosphorylation states of the PTS components change depending on the availability of PTS sugar substrates (20). In this way, the PTS monitors nutritional changes in the environment and plays multiple regulatory roles in various metabolic processes, in addition to sugar transport (16, 21).

In this study, we show that Rsd interacts with SpoT and activates its (p)ppGpp hydrolase activity in *E. coli*. Only the dephosphorylated form of HPr inhibits the formation of the Rsd–SpoT complex and thus antagonizes the effect of Rsd on the (p)ppGpp hydrolase activity of SpoT. We propose that Rsd functions as a regulator for the intracellular concentration of (p)ppGpp through direct interaction with SpoT, and this interaction is involved in the stringent response to a nutrient downshift from a preferred carbon source to a less preferred one.

Results

Interaction of SpoT with Rsd. Several reasons led us to explore the possibility that Rsd might have a specific role other than as an antagonist of the house-keeping σ factor σ^{70} in *E. coli*. First, cellular levels of Rsd have been measured to be lower than that of σ^{70} (17, 22, 23), indicating that Rsd may reduce but not fully antagonize σ^{70} activity. Second, although Rsd was identified as an antagonist of σ^{70} in *E. coli* 20 y ago (17), no obvious phenotype has been observed in *rsd* deletion or overexpression strains to date. Therefore, the importance of Rsd as a σ^{70} antagonist in vivo has still remained elusive. For this reason, we set up a study to explore an in vivo role for Rsd other than what its name implies, and thereby establish a characteristic phenotype associated with the deletion or overexpression of Rsd.

To find a new physiological function of Rsd, we conducted a ligand fishing experiment (16, 24–26) using an N-terminally hexahistidine-tagged Rsd (His-Rsd) as bait. A crude extract of *E. coli* MG1655 grown to stationary phase was mixed with TALON metal-affinity resin (Takara Bio) in the absence or presence of His-Rsd. After brief washes, proteins bound to the resin were eluted with 150 mM imidazole and analyzed by SDS/PAGE and staining with Coomassie brilliant blue. The elution of a protein band for HPr, previously identified as the binding partner of Rsd (16), appearing only in the fraction containing His-Rsd, supports the reliability of this ligand fishing experiment. Noteworthy, another protein band (migrating at apparent molecular mass of ∼80 kDa) was also significantly enriched in the fraction containing His-Rsd (Fig. 1*A*). Peptide mapping of the in-gel tryptic digests revealed that the digested band corresponded to SpoT, the bifunctional (p)ppGpp synthase/hydrolase (27).

To confirm the specific interaction between SpoT and Rsd, GST was fused to the N terminus of SpoT because the native form of SpoT was barely soluble when expressed from a plasmid. The crude extract containing the overexpressed GST–SpoT fusion protein was mixed with various amounts of purified Rsd and each mixture was incubated with TALON resin. After brief washes, proteins bound to the resin were eluted with 150 mM imidazole and analyzed by SDS/PAGE and Coomassie brilliant blue staining. As shown in *SI Appendix*, Fig. S1*A*, a concentration-dependent interaction of Rsd with the GST–SpoT fusion protein was observed, indicating a specific interaction between the two proteins in vitro.

To test whether the interaction between SpoT and Rsd occurs in vivo, we performed bacterial two-hybrid (BACTH) assays (28), which use the reconstitution of the activity of split *Bordetella pertussis* adenylate cyclase CyaA in the *cya*-deficient *E. coli* strain BTH101. When protein–protein interactions were assayed in this strain cotransformed with both plasmids harboring T18 and T25 fusions, full-length SpoT showed a strong interaction with Rsd in both vector combinations (Fig. 1 *B* and *C*). While the BTH101 strain coexpressing T18-SpoT and T25-Rsd hybrid proteins exhibited high β-galactosidase activity, those coexpressing T18 and T25, T18-SpoT and T25, and T18 and T25-Rsd did not develop blue color on 5-bromo-4-chloro-3-indolyl-β-D-galactopyranoside (X-gal) plates (*SI Appendix*, Fig. S1*B*). These data indicate that Rsd interacts with SpoT both in vitro and in vivo.

Interaction of Rsd with the TGS Domain of SpoT. SpoT consists of an N-terminal enzymatic domain (NTD) and a C-terminal domain (CTD) (Fig. 1*B*). The enzymatic domain is composed of a (p)ppGpp hydrolase domain and a (p)ppGpp synthetase domain and it has been suggested that these enzyme activities are controlled by a C-terminal regulatory domain (29, 30). However, the regulation mechanism of SpoT activity in response to diverse starvation stresses remains largely unknown. It has been suggested that the CTD is involved in the regulation of SpoT activities, probably by ligand binding, by modification of the protein folding, or by both (31). The TGS region of the CTD consists of ∼50 amino acid residues and is predicted to predominantly carry a β-sheet structure, which has been named after three protein families containing it (threonyl-tRNA synthetase, "T"; Obg family of GTPases, "G"; and SpoT, "S") (32–34). Acyl carrier protein (ACP) was shown to stimulate the (p)ppGpp synthetase activity of SpoT by directly interacting with the TGS domain (31).

To determine the domain(s) of SpoT required for the interaction with Rsd, we constructed several truncated fragments of SpoT fused to the T25 domain of *B. pertussis* adenylate cyclase (Fig. 1*B*). Each SpoT fragment fused to the T25 domain was coexpressed with Rsd fused to the T18 domain (T18-Rsd) in the *cya*-deficient *E. coli* strain BTH101 and their interactions were assessed by measuring β-galactosidase activity (Fig. 1*C*). While Rsd interacted with the CTD of SpoT (SpoTC1), little interaction was detected with the NTD (SpoTN1). To pinpoint the domain in the CTD of SpoT that interacts with Rsd, we examined the interaction of Rsd with two more nonoverlapping fragments of SpoT: one consisting of the NTD and the TGS domain (construct SpoTN2; amino acids 1–447) and the other corresponding to the CTD lacking the TGS domain (construct SpoTC2; amino acid 448–702), both fused to the T25 domain. While Rsd interacted with SpoTN2, no interaction was detected with SpoTC2. These data suggest that the TGS domain of SpoT is necessary for the interaction with Rsd.

The TGS domain-dependent interaction between Rsd and SpoT was further confirmed using metal affinity pull-down assays with His-Rsd and crude extracts of *E. coli* cells overexpressing the truncated constructs SpoTN2 and SpoTC1 (*SI Appendix*, Fig. S2). As the amount of His-Rsd increased, the amounts of pulled down SpoTN2 and SpoTC1 proteins also increased. Together, these data confirm that Rsd interacts with the TGS domain of SpoT. However, we have not been able to test the direct interaction of Rsd with the TGS domain alone, because expression of the TGS domain itself has been unsuccessful, even after repeated attempts.

RelA and SpoT share a similar domain organization and significant amino acid sequence identity (∼31% throughout the entire protein) in *E. coli*. While both of them possess (p)ppGpp synthetase activity, the most conserved region between the two proteins corresponds to the TGS domain, with ∼52% amino acid sequence identity with each other, rather than the synthetase domain (∼50% identity). To examine whether RelA can also interact with Rsd through its TGS domain, RelA was fused

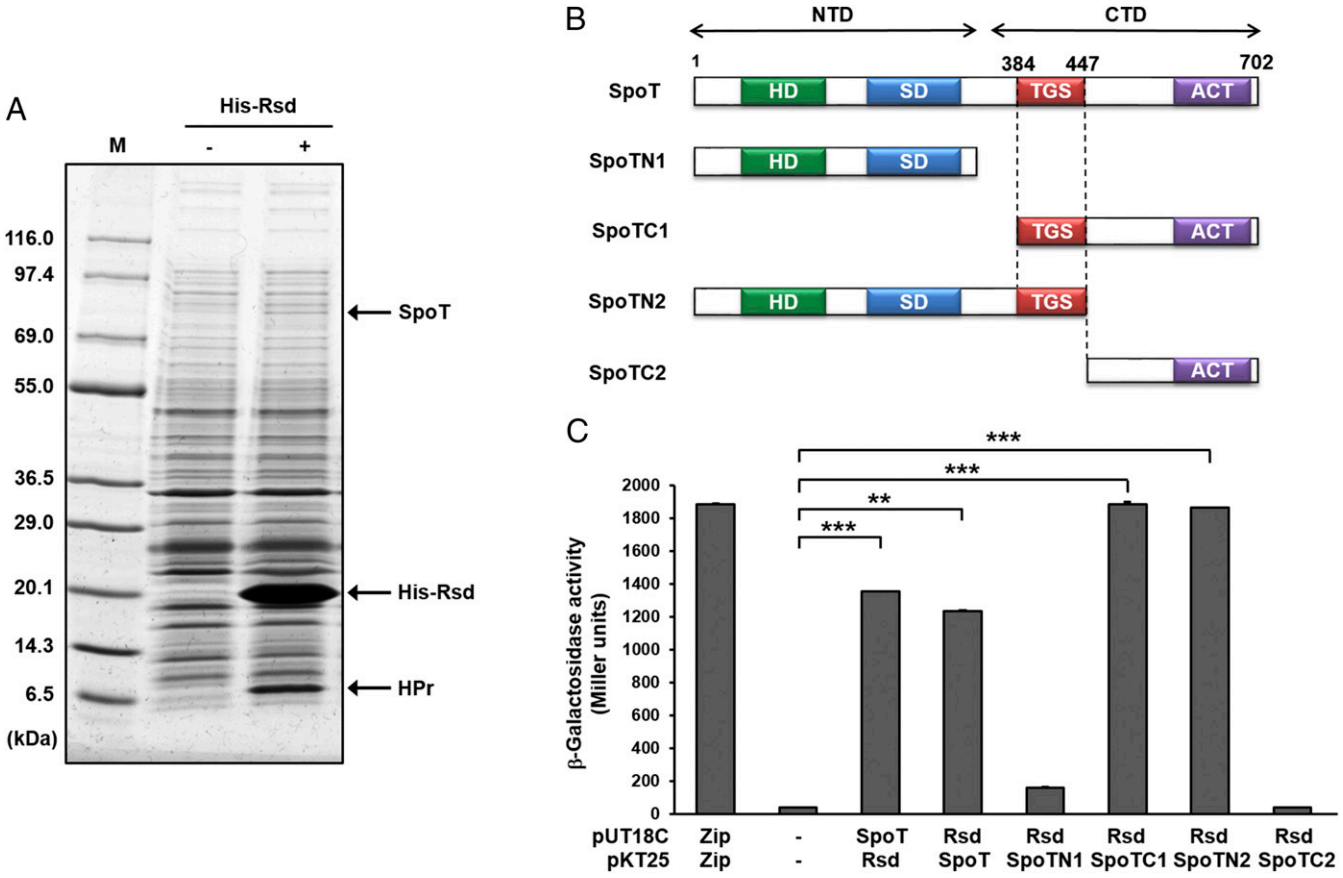

Fig. 1. Interaction of Rsd with SpoT. (*A*) Ligand fishing experiment was carried out to search for proteins specifically interacting with Rsd. Crude extract prepared from *E. coli* strain MG1655 was mixed with (lane +) or without (lane –) 150 μg of purified His-Rsd. Each mixture was incubated with 50 μL TALON resin for metal-affinity chromatography. Proteins bound to each column were analyzed as described in *Materials and Methods*. Protein bands bound specifically to His-Rsd are indicated by arrows. Lane M refers to the molecular mass markers (KOMA Biotech). (*B*) A schematic diagram of SpoT and its truncated forms. HD domain indicates ppGpp hydrolase domain; SD domain, ppGpp synthetase domain; TGS domain named for three protein families containing it (threonyl-tRNA synthetase, Obg family of GTPases, and SpoT); ACT domain, named after aspartokinase, chorismate mutase and TyrA. (*C*) Quantitative BACTH assays to assess the in vivo interaction of Rsd with SpoT. β-Galactosidase activity was measured with permeabilized cells cotransformed with derivatives of pUT18C and pKT25 as indicated by direct enzyme assay (Miller units). Zip, the leucine zipper domain of *Saccharomyces cerevisiae* GCN4, served as a positive control. The mean and standard deviation of three independent measurements are shown. Statistical significance was determined using Student's *t* test (**$P < 0.005$ and ***$P < 0.001$).

to the T25 domain (T25-RelA) and the resulting hybrid protein was tested in two-hybrid assays with T18-Rsd (*SI Appendix*, Fig. S3*A*). While the BTH101 strain coexpressing T18-Rsd and T25-SpoT showed a significantly higher β-galactosidase activity than the negative control coexpressing T18 and T25, the strain coexpressing T18-Rsd and T25-RelA did not produce β-galactosidase. This result suggests that Rsd specifically interacts with SpoT. It is interesting to note that ACP also interacts with the TGS domain of SpoT but not with that of RelA in *E. coli* (31).

Enzyme IIA^{Ntr} of the nitrogen PTS was previously shown to interact with SpoT in *Ralstonia eutropha*, the ortholog of *E. coli* SpoT protein (35), and a single RelA/SpoT homolog protein of *Caulobacter crescentus* (36). Rsd has a similar molecular mass and pI (18.24 kDa and 5.65, respectively) to $EIIA^{Ntr}$ (17.96 kDa and 5.57, respectively) in *E. coli*. Therefore, we wanted to test whether the interaction of $EIIA^{Ntr}$ with SpoT also occurs in *E. coli*. Because SpoTC1 showed a relatively higher solubility than other SpoT constructs, we used SpoTC1 to study its interaction with $EIIA^{Ntr}$. The crude extract overexpressing the truncated construct SpoTC1 was mixed with various amounts of purified Rsd or $EIIA^{Ntr}$ and incubated with TALON resin. To the mixture containing $EIIA^{Ntr}$, pyruvate was added to dephosphorylate or PEP to phosphorylate $EIIA^{Ntr}$. After brief washes, proteins bound to the resin were eluted with 150 mM imidazole and analyzed by SDS/PAGE and Coomassie brilliant blue staining. As shown in *SI Appendix*, Fig. S3*B*, SpoTC1 interacted with Rsd but not with $EIIA^{Ntr}$, regardless of its phosphorylation state. The interaction between $EIIA^{Ntr}$ and full-length SpoT was also tested in vivo by BACTH assays (*SI Appendix*, Fig. S3*A*). Neither of wild-type $EIIA^{Ntr}$, its phosphomimetic (H73E) and dephosphomimetic mutant (H73A) could interact with SpoT, indicating that the SpoT–Rsd interaction is specific in *E. coli*. Our data also suggest that stress signals and regulatory mechanisms for the stringent response could be diverse among microorganisms, consistent with the previous report (35).

Activation of the (p)ppGpp Hydrolase Activity of SpoT by Rsd. Because Rsd specifically interacts with SpoT through the TGS domain, we predicted that Rsd could regulate the catalytic activity of SpoT. The (p)ppGpp hydrolysis function of SpoT is critical for balancing cellular (p)ppGpp concentrations in the stringent (*relA*$^+$) strains, and therefore disruption of the *spoT* gene is lethal in *E. coli relA*$^+$ strains (7). Thus, we first tested the effect of Rsd on the ppGpp hydrolase activity of SpoT by measuring the amounts of hydrolyzed ppGpp and produced GDP using high-performance liquid chromatography (HPLC). As

shown in Fig. 2*A*, GST–SpoT hydrolyzed ppGpp to GDP in vitro, with the K_m and K_{cat} values of SpoT for ppGpp being 24.48 μM and 3.38 min^{-1}, respectively (*SI Appendix*, Fig. S4 *A* and *B*). The K_m value is well within the physiological ppGpp concentrations given that the cellular level of ppGpp corresponds to 1 mM during the stringent response (37). Interestingly, the ppGpp hydrolase activity of SpoT increased with the addition of Rsd but not by the same amount of BSA, a known carrier protein. Rsd alone did not show ppGpp hydrolase activity, indicating no contamination with SpoT during purification of Rsd. Therefore, these data suggest that Rsd activates the ppGpp hydrolase activity of SpoT by direct interaction in vitro.

As shown in *SI Appendix*, Fig. S4*C*, the stimulatory effect of Rsd on the SpoT ppGpp hydrolase activity appeared to be concentration-dependent and saturable. The concentration of Rsd required for half-maximum stimulation of the ppGpp hydrolase activity ($K_{0.5}$) was ~3.65 μM. This $K_{0.5}$ value corresponds to ~2,200 molecules per cell when calculated assuming an *E. coli* cell volume of 1×10^{-15} L (22). Rsd levels were reported to increase by approximately twofold during stationary phase, with ~6,200 molecules in an *E. coli* cell, compared with the levels in exponentially growing cells (~3,300 molecules per cell) (22). The cellular levels of SpoT are approximately one-tenth of that for Rsd (23). Thus, it is reasonable to assume that regulation of the SpoT ppGpp hydrolase activity by Rsd can occur in vivo, especially in the stationary phase or under stress conditions.

Because (p)ppGpp plays a crucial role in the stringent response to amino acid starvation, strains lacking (p)ppGpp are unable to grow on minimal medium without amino acids (7). Therefore, we assumed that if Rsd stimulates the (p)ppGpp hydrolysis function of SpoT in vivo, increased expression of Rsd might deplete intracellular (p)ppGpp pools, resulting in a growth defect under amino acid starvation conditions. To test this assumption, we compared the growth of *E. coli relA* mutant strains

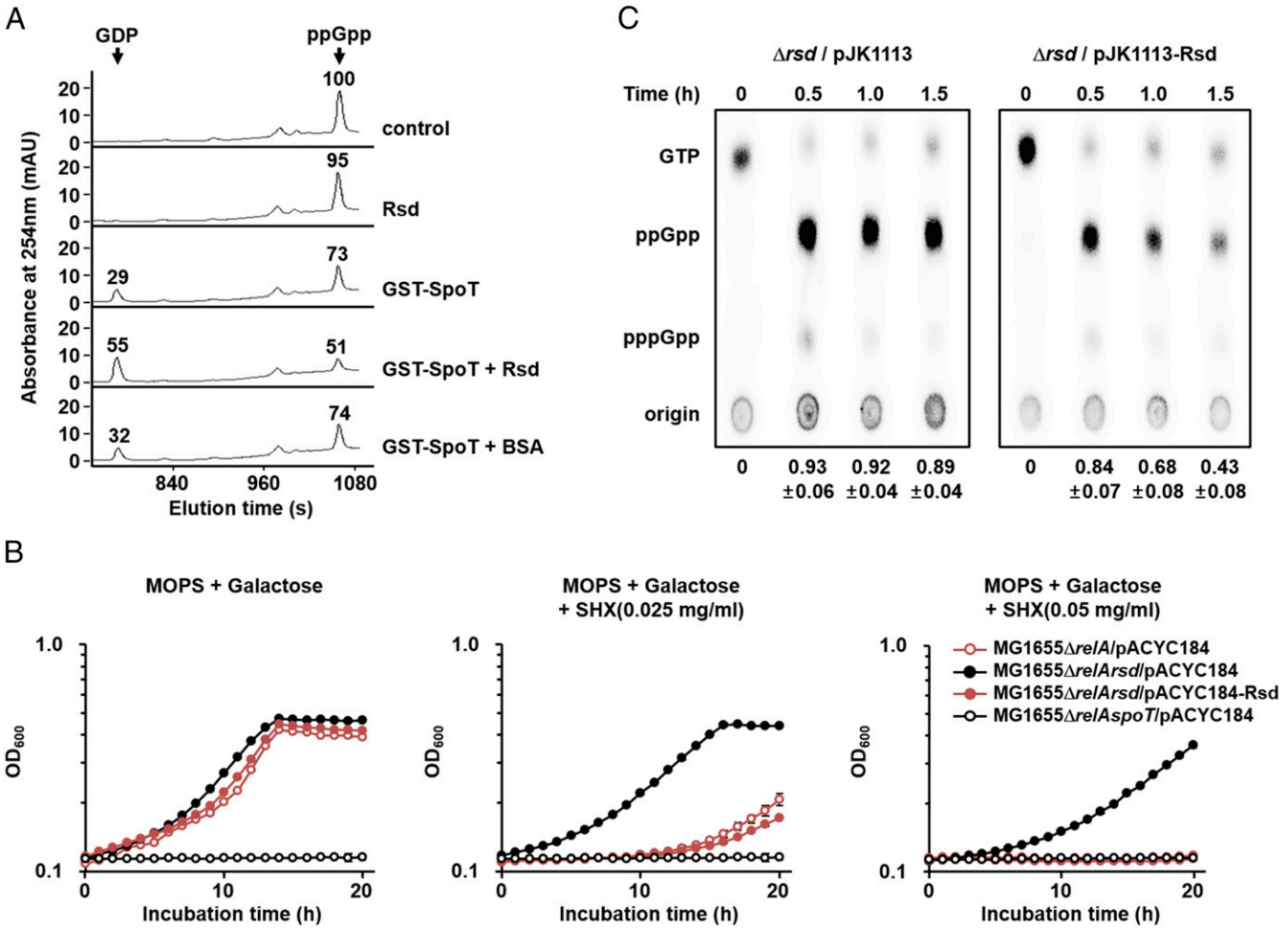

Fig. 2. Activation of the (p)ppGpp hydrolase activity of SpoT by Rsd. (*A*) The stimulatory effect of Rsd on the ppGpp hydrolase activity of SpoT was measured in vitro. The ppGpp hydrolase activity of purified GST-SpoT (3 μg) was assayed in a reaction mixture containing 23.33 μM ppGpp in the presence of purified Rsd or BSA (19 μg each). After incubation at 37 °C for 5 min, the reaction mixtures were applied to a Supelcosil LC-18-T HPLC column (Sigma Aldrich), and ppGpp and GDP were monitored by measuring the absorbance at 254 nm (A_{254}). Relative peak areas are shown above each peak, considering the peak area of ppGpp in the control sample as 100. Representative data from three independent experiments are shown. (*B* and *C*) Activation of the (p)ppGpp hydrolase activity of SpoT by Rsd in vivo. (*B*) Growth curves of *E. coli* strains in MOPS minimal medium (pH 7.2) supplemented with 0.2% galactose in the absence and presence of SHX. After inoculation, 100-μL aliquots of each strain were transferred into a 96-well plate and growth was monitored at 600 nm using a multimode microplate reader (TECAN). The mean and standard deviation of three measurements are shown. (*C*) The MG1655Δ*rsd* strain carrying pJK1113 or pJK1113-Rsd was incubated in low-phosphate MOPS minimal medium containing 0.2% galactose, 0.02% arabinose, and 100 μCi/mL $^{32}PO_4^{3-}$. Exponentially growing cells were treated with SHX (1 mg/mL) and intracellular (p)ppGpp concentrations were analyzed by thin-layer chromatography at the indicated times. Relative amounts of (p)ppGpp were calculated as the intensity of (p)ppGpp divided by that of (p)ppGpp plus GTP. The mean and standard deviation of three independent measurements are shown below each lane.

with different levels of Rsd expression in the absence and presence of serine hydroxamate (SHX), an inhibitor of seryl-tRNA synthetase as a serine homolog (Fig. 2*B*). It is known that the addition of SHX induces serine starvation and thereby the stringent response (38). As expected, an *E. coli relA spoT* double-mutant lacking (p)ppGpp [(p)ppGpp^0 strain] could not grow in MOPS minimal medium with galactose as a sole carbon source in the absence of amino acids, whereas the *relA rsd* double-mutant carrying the control plasmid pACYC184 showed normal growth regardless of the presence of SHX, indicating that the weak (p)ppGpp synthetase activity of SpoT alone is enough to cope with serine starvation. However, the *relA* mutant carrying pACYC184 and the *relA rsd* double-mutant carrying pACYC184-Rsd expressing Rsd from its own promoter (16) had a severe growth defect similar to the (p)ppGpp^0 strain as the SHX concentration increased, while they exhibited a similar growth rate to the *relA rsd* double-mutant carrying pACYC184 in the absence of SHX. These data indicate that Rsd stimulates SpoT-mediated (p)ppGpp hydrolysis in vivo.

While the Rsd(D63A) mutant (substitution of Asp-63 to Ala) was shown unable to interact with and therefore to antagonize the activity of σ^{70} in a previous study (39), this mutant protein could still interact, as tightly as wild-type Rsd, with SpoT (*SI Appendix*, Fig. S5 *A* and *B*), and overexpression of Rsd(D63A) resulted in the same phenotype as overexpression of the wild-type Rsd (*SI Appendix*, Fig. S5*C*). Moreover, no obvious difference in the transcriptional levels of *relA* and *spoT* was detected in *rsd* deletion and overexpression strains (*SI Appendix*, Fig. S6). Thus, we verified that the growth defect of *rsd*$^+$ strains in the *relA* mutant background under amino acid starvation conditions is not due to the anti-σ^{70} activity of Rsd.

To confirm that the effect of Rsd was due to an increase in the (p)ppGpp hydrolase activity of SpoT, we measured the intracellular (p)ppGpp levels (Fig. 2*C*). A robust induction of (p)ppGpp synthesis was observed in both *rsd* deletion and overexpression strains 30 min after the addition of SHX, indicating that induction of the stringent response by SHX is little affected by the expression level of Rsd. However, the cellular levels of (p)ppGpp decreased much more rapidly in the *rsd* mutant strain carrying pJK1113-Rsd than in the same strain carrying pJK1113, indicating that Rsd stimulates the hydrolysis of (p)ppGpp in vivo. This observation explains that the growth defect of *rsd*$^+$ strains under SHX-induced serine starvation (Fig. 2*B*) is due to the increased degradation of (p)ppGpp.

The Stimulatory Effect of Rsd on the (p)ppGpp Hydrolase Activity of SpoT Is Blocked by Dephosphorylated HPr. In a previous study, we showed that HPr, a general component of the sugar PTS, is predominantly dephosphorylated during glucose transport and

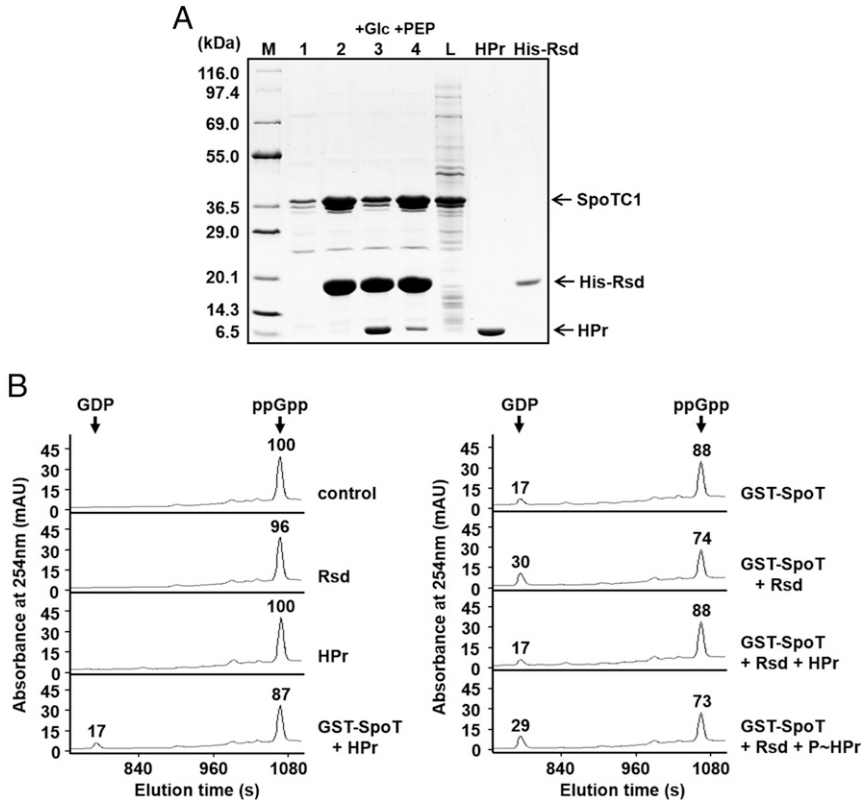

Fig. 3. The stimulatory effect of Rsd on the SpoT ppGpp hydrolase activity is abolished by dephosphorylated HPr. (*A*) Interference of the Rsd–SpoT complex formation by a dephosphorylated form of HPr. To test the effect of the phosphorylation state of HPr on the formation of the Rsd–SpoT complex, an *E. coli* cell extract expressing SpoTC1 was mixed with binding buffer (lane 1), 170 μg His-Rsd (lane 2), or a mixture of 170 μg His-Rsd, 240 μg HPr, and 2 μg EI (lanes 3 and 4), and HPr was dephosphorylated by adding 2 mM glucose (lane 3) or phosphorylated by adding 2 mM PEP (lane 4). Each mixture was incubated with 50 μL TALON resin for metal-affinity chromatography. After elution with imidazole, proteins bound to each TALON resin were analyzed by SDS/PAGE and Coomassie blue staining. Lane M, molecular mass markers; lane L, *E. coli* cell lysate expressing SpoTC1 before metal-affinity chromatography. Purified HPr and His-Rsd were also run as a control. (*B*) Stimulation of the SpoT ppGpp hydrolase activity by Rsd is blocked by the dephosphorylated form of HPr. The ppGpp hydrolase activity of purified GST–SpoT (2.5 μg) was assayed in a reaction mixture containing 38.49 μM ppGpp in the presence of different combinations of Rsd (15.6 μg) and HPr (28 μg), as indicated. HPr was phosphorylated by adding EI and 2 mM PEP (P~HPr). After incubation at 37 °C for 5 min, the reaction mixture was applied to a Supelcosil LC-18-T HPLC column, and ppGpp and GDP were monitored by measuring the A_{254}. Relative peak areas are shown above each peak, considering the peak area of ppGpp in the control sample as 100. Representative data from three independent experiments are shown.

only dephosphorylated HPr interacts with Rsd to antagonize its activity (16, 21, 40). We therefore expected that the Rsd–SpoT interaction could be affected by the phosphorylation state of HPr, resulting in changes in the intracellular level of (p)ppGpp. To verify this assumption, we first examined the effect of the phosphorylation state of HPr on formation of the Rsd–SpoT complex by pull-down assays under various conditions (Fig. 3*A*). After the *E. coli* cell lysate containing overexpressed SpoTC1 was mixed with purified His-Rsd alone or together with HPr and EI, this mixture was incubated either with glucose to dephosphorylate or with PEP to phosphorylate HPr. Then each mixture was incubated with TALON resin for metal-affinity chromatography. After brief washes, proteins bound to the resin were eluted and analyzed by SDS/PAGE (Fig. 3*A*). The amount of eluted SpoTC1 significantly increased in the presence of His-Rsd, supporting the specific interaction of SpoTC1 with Rsd (compare lanes 1 and 2 in Fig. 3*A*). When the mixture of the SpoTC1 lysate and His-Rsd was incubated with HPr and glucose (thus HPr dephosphorylated), the amount of SpoTC1 bound to Rsd significantly decreased with a concomitant increase in the amount of HPr bound to His-Rsd (compare lanes 2 and 3 in Fig. 3*A*). However, when the same mixture was incubated with HPr and PEP (and thus HPr phosphorylated), formation of the Rsd-SpoTC1 complex was little affected by HPr (lane 4 in Fig. 3*A*). These data indicate that only the dephosphorylated form of HPr can interact with Rsd and sequesters it from SpoTC1. We then tested the effect of HPr on the stimulation of the SpoT ppGpp hydrolase activity by Rsd in vitro using HPLC (Fig. 3*B*). Interestingly, whereas dephosphorylated HPr apparently inhibited the stimulatory effect of Rsd on the ppGpp hydrolysis by SpoT, phosphorylated HPr did not.

We also determined the effect of dephosphorylated HPr on the cellular level of (p)ppGpp in vivo (*SI Appendix*, Fig. S7). Consistent with the data in Fig. 2*C*, the level of (p)ppGpp decreased more rapidly in the Rsd-overexpressing strain than in the *rsd*-deficient strain. However, the (p)ppGpp hydrolysis rate was significantly lower in the strain coexpressing Rsd and unphosphorylatable HPr(H15A), compared with that in the strain overexpressing Rsd alone. These results suggest that HPr of the sugar PTS can influence the formation of the Rsd–SpoT complex and thereby regulate the cellular level of (p)ppGpp depending on its phosphorylation state in vivo.

Regulation of (p)ppGpp Hydrolase Activity of SpoT by Rsd Is Dependent on Carbon Sources. We have previously shown that the phosphorylation state of HPr is determined by sugars supplemented to the medium (16, 24). As shown in Fig. 4*A*, HPr was mostly dephosphorylated in the presence of glucose or *N*-acetylglucosamine, whereas it was predominantly phosphorylated in the presence of galactose or glycerol. Therefore, we assumed that the (p)ppGpp level would be less, since the concentration of free Rsd should be higher, thus cells might be more sensitive to the SHX-induced serine starvation in the presence of galactose or glycerol than in the presence of glucose or *N*-acetylglucosamine. To verify this assumption, we constructed a *relA rsd* double-mutant, and transformed this mutant with the low copy-number plasmid pACYC184 (as a control) or the plasmid pACYC-Rsd expressing Rsd from its own promoter, in an attempt to examine only the direct effects of Rsd on the SpoT-triggered stringent response

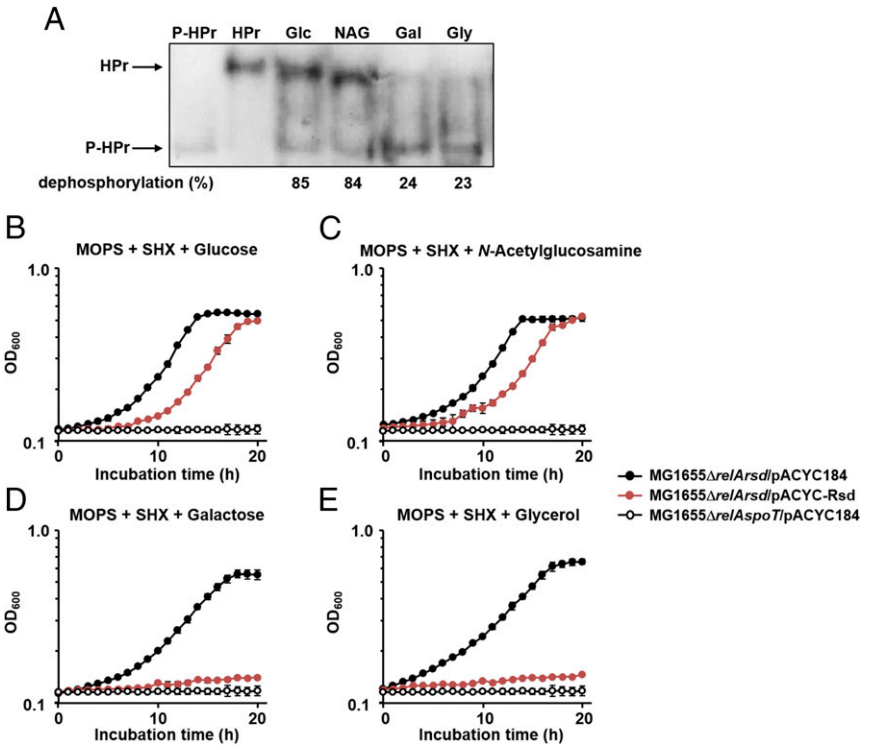

Fig. 4. Sugar source dependence of the phosphorylation state of HPr and the stimulatory effect of Rsd on the SpoT (p)ppGpp hydrolase activity. (*A*) Determination of the in vivo phosphorylation state of HPr. The phosphorylation state of HPr was determined in the *E. coli* strain MG1655/pACYC-HPr grown in LB medium containing the indicated sugars as described in *Materials and Methods*. Purified HPr (3.5 ng) was used as a positive control. Band intensities were analyzed using ImageJ software. The percentages of dephosphorylated HPr over total HPr are shown below the gel. Gal, galactose; Glc, glucose; Gly, glycerol; NAG, *N*-acetylglucosamine. (*B*–*E*) Growth curves of *E. coli* strains treated with SHX (0.025 mg/mL) in MOPS minimal medium (pH 7.2) supplemented with 0.2% glucose (*B*), *N*-acetylglucosamine (*C*), galactose (*D*), or glycerol (*E*). After inoculation, 100-μL aliquots of each strain were transferred into a 96-well plate and growth was monitored at 600 nm using a multimode microplate reader (TECAN). The mean and standard deviation of three measurements are shown.

depending on carbon sources. Thus, the growth patterns of these strains were compared in the presence of various carbon sources with or without SHX (Fig. 4 *B*–*E* and *SI Appendix*, Fig. S8). While the *relA spoT* double-mutant [(p)ppGpp^0] strain carrying pACYC184 showed a severe growth defect in MOPS medium containing glucose, *N*-acetylglucosamine, galactose, or glycerol as the sole carbon source regardless of the presence of SHX, the *relA rsd* double-mutant carrying pACYC184 exhibited normal growth regardless of the supplemented carbon source, although the addition of SHX caused some growth retardation (compare Fig. 4 and *SI Appendix*, Fig. S8). Expression of Rsd from its own promoter on pACYC-Rsd caused a slight but not significant growth retardation of the *relA rsd* double-mutant compared with the same strain carrying pACYC184, regardless of the supplemented carbon sources in MOPS medium in the absence of SHX (*SI Appendix*, Fig. S8). Interestingly, however, growth of the *relA rsd* double-mutant expressing Rsd was significantly inhibited by SHX in the presence of galactose or glycerol as the sole carbon source, to a similar level to that of the (p)ppGpp^0 strain carrying pACYC184 (Fig. 4 *D* and *E*), whereas the same strain showed only moderate growth retardation compared with the *relA rsd* double-mutant carrying pACYC184 when glucose or *N*-acetylglucosamine was supplemented as the sole carbon source (Fig. 4 *B* and *C*). These data suggest that the carbon source can influence the stringent response by regulating the stimulatory effect of Rsd on the SpoT (p)ppGpp hydrolase activity through altering the phosphorylation state of HPr in vivo.

Rsd Regulates the Stringent Response During Carbon Source Downshift. Microorganisms face the constant challenge of fluctuating conditions in their natural environments, such as nutrient shifts. On exposure to nutrient downshifts, the cellular concentration of (p)ppGpp displays an abrupt increase followed by a gradual decrease (41). This mechanism of balancing the (p)ppGpp level by stimulating the hydrolase activity of SpoT appears to be important because the uncontrolled accumulation of (p)ppGpp is lethal (42). Because the stimulatory effect of Rsd on SpoT (p)ppGpp hydrolase activity is mediated by the type and availability of carbon sources, we assumed that Rsd may function in response to a carbon source downshift from a preferred carbon source to a less-preferred one. When *E. coli* is cultured on a mixture of various carbon sources, glucose is preferentially utilized by inhibiting the consumption of other carbon sources (43). Once glucose is depleted, growth is transiently arrested and (p)ppGpp accumulates rapidly in the cell (44). As a result, the accumulated (p)ppGpp controls regulatory networks that coordinate resumption of growth (45). Considering that the phosphorylation state of HPr is determined by the availability of preferred PTS sugars, such as glucose (16, 24) (Fig. 4*A*), it seems reasonable to assume that (p)ppGpp levels need to be reduced before growth can resume during a carbon source downshift, and this explains the requirement of Rsd for the stimulation of SpoT-catalyzed (p)ppGpp hydrolysis.

To verify this assumption, we examined the effect of Rsd on the diauxic shift of *E. coli* cells during growth in the medium supplemented with 0.02% glucose and 0.1% casamino acids (Fig. 5). To rule out the effect of amino acid starvation during the diauxic shift and to assess only the effect of the carbon downshift, casamino acids were added at a much higher concentration than glucose. All strains showed similar growth curves during the glucose consumption period, and then transient growth arrest after glucose was exhausted. As shown in Fig. 5, the *rsd* mutant carrying pACYC184 (Fig. 5, red triangles), had a longer diauxic lag and showed less-efficient growth on casamino acids than the wild-type strain carrying pACYC184 (Fig. 5, black circles). The lag time and growth of the *rsd* mutant was restored by complementation with pACYC-Rsd (Fig. 5, gray squares) or pACYC-Rsd(D63A) (Fig. 5, white diamonds), indicating that the phenotype of the *rsd* mutant is not due to loss of the anti-σ^{70} activity. Because the (p)ppGpp level was previously shown to increase in a RelA-dependent manner during a nutrient downshift in *E. coli* (41, 46), we examined whether Rsd is required to balance the

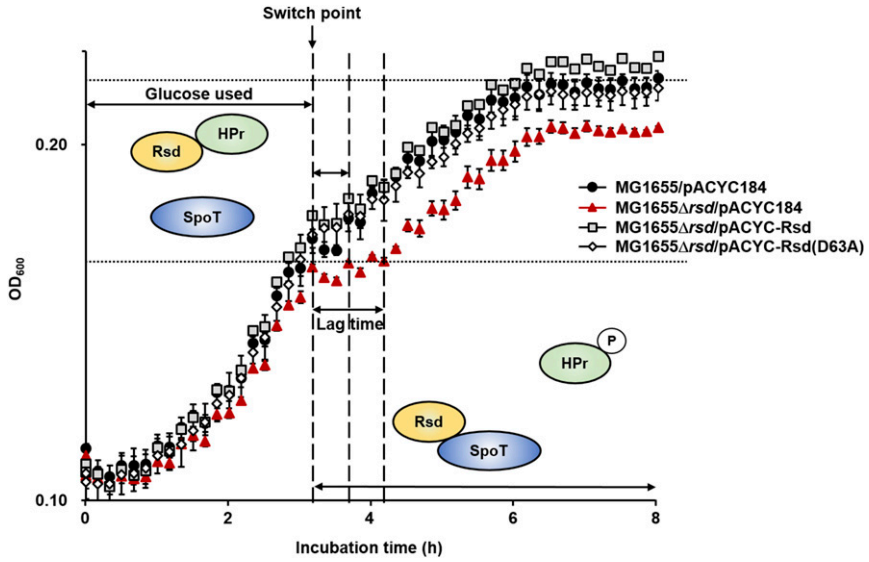

Fig. 5. Implication of Rsd during a carbon source downshift. Growth curves were measured during a carbon downshift from glucose to casamino acids. Cells grown overnight in LB medium were harvested, washed, suspended in MOPS minimal medium containing 0.1% casamino acids and 0.02% glucose. Then, 100-μL aliquots of each strain were transferred into a 96-well plate and growth was monitored at 600 nm using a multimode microplate reader (TECAN). The mean and standard deviation of three measurements are shown. In the presence of glucose, HPr is predominantly dephosphorylated and then sequesters Rsd from SpoT to maintain the (p)ppGpp hydrolytic activity at basal levels. On depletion of glucose, however, the ppGpp level abruptly increases in *relA*$^+$ strains. Therefore, the (p)ppGpp hydrolase activity of SpoT needs to be stimulated to counterbalance the RelA-dependent large accumulation of (p)ppGpp. This appears to be achieved by phosphorylation of HPr. Because phospho-HPr cannot interact with Rsd, Rsd can bind and activate the (p)ppGpp hydrolase activity of SpoT to balance the intracellular (p)ppGpp concentrations, which contributes to the growth resumption of *E. coli* cell during a carbon downshift.

RelA-mediated (p)ppGpp accumulation. While the *rsd*-deficient mutant showed a longer diauxie lag than the wild-type strain, the *relA* mutant strain exhibited a remarkably decreased lag time (*SI Appendix*, Fig. S9). In addition, the effect of *rsd* deletion disappeared in the *relA* mutant background, indicating that Rsd counterbalances the RelA-dependent accumulation of (p)ppGpp by stimulating the (p)ppGpp hydrolase activity of SpoT during a carbon downshift. The effect of the *rsd* mutation on the growth of *E. coli* was also examined during the carbon source downshift from glucose to succinate (*SI Appendix*, Fig. S10). An *rsd*-deficient mutant exhibited a longer diauxic lag and showed less efficient growth on succinate than the wild-type strain. These results suggest that Rsd functions as a direct link between the PTS-dependent diauxic shift and the SpoT-mediated stringent response. We also identified a distinct phenotype of an *rsd* mutant associated with the stringent response which is independent of its anti-σ^{70} activity.

Discussion

The activities of RelA and SpoT are regulated by different stress signals. While RelA possessing only (p)ppGpp synthetic activity responds primarily to amino acid starvation, SpoT having both (p)ppGpp synthetic and hydrolytic activities functions as a hub protein that integrates various stress signals including fatty acid, phosphate, iron, and carbon source starvation (13). Because the hydrolytic activity of SpoT is crucial for balancing cellular (p)ppGpp concentrations, disruption of the *spoT* gene is lethal in *relA*-proficient *E. coli* strains due to the accumulation of too much (p)ppGpp (7, 47). It was recently revealed that the enzymatic activity of RelA is also activated by ppGpp itself (48). This positive allosteric feedback regulation mechanism also supports the importance of the SpoT-mediated (p)ppGpp hydrolysis in relaxing the stringent response.

There have been a few studies on the regulation of the SpoT activity through protein–protein interactions. ObgE was previously shown to interact with SpoT to maintain the low level of (p)ppGpp under normal growth conditions (49). However, a more recent study has shown that the effect of ObgE overexpression on the intracellular level of (p)ppGpp is negligible (50). Similarly, the *obgE* deletion mutant did not show an increase in the (p)ppGpp level as opposed to previous findings, suggesting that ObgE is not responsible for the regulation of SpoT activity in vitro and in vivo (51). ACP has also been shown to interact with SpoT to stimulate the (p)ppGpp synthetase activity of SpoT in response to fatty acid starvation (31). A direct interaction of SpoT with enzyme IIA^{Ntr} of the nitrogen-related PEP-dependent phosphotransferase system has been reported in *R. eutropha* (35) and *C. crescentus* (36), but these interactions appeared to inhibit SpoT (p)ppGpp hydrolase activity.

However, despite the physiological importance, little is known about the molecular mechanism stimulating the (p)ppGpp hydrolase activity of SpoT in *E. coli*. In this study, we demonstrate that Rsd directly interacts with SpoT to stimulate its (p)ppGpp hydrolase activity both in vitro and in vivo (Figs. 1 and 2). As expected from the fact that Rsd can form a tight complex only with the dephosphorylated form of HPr (16, 21) and that the phosphorylation state of HPr can be changed by the type of sugar available in the medium (16, 24), the stimulatory effect of Rsd on SpoT (p)ppGpp hydrolase activity was influenced by the sugar source supplemented (Fig. 4 and *SI Appendix*, Fig. S8). Thus, this study provides an example of a regulator stimulating SpoT (p)ppGpp hydrolase activity and an example of a direct link between the sugar PTS and the stringent response. The TGS domain of SpoT functions as the site for Rsd binding (Fig. 1*C* and *SI Appendix*, Fig. S2) as well as for acyl-ACP binding (31). Recently, the TGS domain of RelA has been shown to be the site for recognition of charged or uncharged CCA ends of cognate tRNA (6, 52). Given these pivotal roles of the TGS domain, this domain appears to be a regulatory link between carbon, lipid, and amino acid metabolism, and the stringent response.

Although Rsd was identified as an antagonist of σ^{70} in *E. coli* (17), no obvious phenotype has been observed in *rsd* deletion or overexpression strains to date. However, we showed that the overproduction of Rsd significantly decreased the intracellular (p)ppGpp levels (Fig. 2*C*). Moreover, the *relA* mutant strains expressing Rsd exhibits severe growth defects under SHX-induced stress condition similar to that of the *relA spoT* double mutant [$(p)ppGpp^0$] strain (Fig. 2*B*). Furthermore, the *rsd* mutant showed a longer diauxic lag and less-efficient growth during the carbon source downshift from glucose to casamino acids or succinate (Fig. 5 and *SI Appendix*, Fig. S10) than the wild-type strain. We confirmed that these growth characteristics of both the Rsd-overexpressing and *rsd*-deficient strains were not associated with the anti-σ^{70} activity of Rsd but with its stimulation of the SpoT (p)ppGpp hydrolase activity (Fig. 5 and *SI Appendix*, Fig. S5). Therefore, this study provides clear genotype–phenotype correlations in both Rsd overexpression and deletion strains.

Considering its critical role in the stringent response, the (p)ppGpp hydrolase activity of SpoT must be tightly regulated to ensure that it is stimulated only when necessary. Under good carbon conditions, the intracellular (p)ppGpp concentrations are maintained at a low level (53). Thus, stimulation of the SpoT (p)ppGpp hydrolase activity is unnecessary. When cells are growing on glucose, HPr is dephosphorylated and sequesters Rsd so that the (p)ppGpp hydrolase activity of SpoT will be maintained at a basal level. However, when glucose is exhausted, the (p)ppGpp level abruptly increases in a RelA-dependent manner to efficiently coordinate gene expression necessary to resume growth on poor carbon sources (41). However, uncontrolled accumulation of (p)ppGpp can cause severe growth inhibition (42) or cell death (54). Therefore, sophisticated control of SpoT-mediated (p)ppGpp hydrolysis is necessary to balance the intracellular (p)ppGpp concentrations. This can be achieved by phosphorylation of HPr. When cells are transited to poor carbon conditions, such as casamino acids or succinate, HPr is predominantly phosphorylated and thus Rsd can interact with and stimulate the SpoT-catalyzed (p)ppGpp hydrolysis to counterbalance the RelA-catalyzed synthesis (Fig. 5 and *SI Appendix*, Figs. S9 and S10). In this way, the intracellular level of (p)ppGpp can be adjusted to allow *E. coli* to adapt to carbon source fluctuations. Therefore, Rsd functions as a direct link between the PTS-dependent diauxic shift and the SpoT-mediated stringent response.

Materials and Methods

Bacterial Strains, Plasmids, and Culture Conditions. The bacterial strains, plasmids, and oligonucleotides used in this study are listed in *SI Appendix*, Tables S1 and S2. Bacterial cells were grown at 37 °C in LB medium or MOPS minimal medium (pH 7.2) supplemented with the indicated carbon sources. All plasmids were constructed using standard PCR-based cloning procedures and verified by sequencing. In-frame deletion mutants used in this study were constructed using the pKD46 plasmid, as previously described (55). The *relA* gene was replaced by the kanamycin-resistance gene and the *spoT* gene was replaced by the chloramphenicol-resistance (*cat*) gene or streptomycin-resistance gene.

To construct pJK1113-HPr(H15A), the *bla* gene in pJK1113 was replaced with the *cat* gene as described previously (56). The *cat* gene PCR product and the linearized PCR product of pJK1113 were combined using the EZ-Fusion Cloning kit (Enzynomics). Then, the *ptsH* promoter and ORF (His15 to Ala) amplified by PCR from pACYC-HPr(H15A) (24) using the primers RS953 and RS954 (*SI Appendix*, Table S2) were digested with SalI and inserted into the corresponding site of pJK1113.

Purification of Overexpressed Proteins. Purification of EI and HPr was accomplished using MonoQ 10/100 GL and HiLoad 16/60 Superdex 75 prepgrade columns (GE Healthcare Life Sciences) as recently reported (16, 24, 57), and Rsd was purified in a similar manner. His-tagged protein (His-Rsd) was purified using TALON metal-affinity resin according to the manufacturer's

instructions (Takara Bio). The protein was eluted with the binding buffer (20 mM Hepes-NaOH, pH 7.6, 100 mM NaCl, 5 mM β-mercaptoethanol, and 5% glycerol) containing 150 mM imidazole. The fractions containing His-Rsd were concentrated using Amicon Ultracel-3K centrifugal filters (Merck Millipore). To obtain homogeneous His-tagged protein (>98% pure) and to remove imidazole, the concentrated pool was chromatographed on a HiLoad 16/60 Superdex 75 prepgrade column equilibrated with the binding buffer. The purified protein was stored at −80 °C until use. GST-tagged protein (GST–SpoT) was purified using Glutathione-S-agarose beads (Sigma Aldrich) according to the manufacturer's instructions. The protein was eluted with the binding buffer containing 10 mM reduced glutathione (GSH). The fractions containing GST–SpoT was concentrated using Amicon Ultracel-3K centrifugal filters. To remove GSH and to purify the protein to homogeneity (<95% purity), the concentrated pool was dialyzed against a large volume of GSH-free buffer (50 mM Tris·HCl, pH 8, 270 mM potassium acetate, 5% glycerol, and 10 mM DTT).

Ligand Fishing Experiments Using Metal-Affinity Chromatography. *E. coli* MG1655 cells grown overnight in LB medium were harvested and resuspended in the binding buffer. Cells were disrupted by two passages through a French pressure cell at 10,000 psi. After centrifugation at 100,000 × *g* for 25 min at 4 °C, the supernatant was divided into aliquots and mixed either with a His-tagged protein as bait or with binding buffer as a control. Each mixture was then incubated with 50 μL TALON metal affinity resin in a 1.5-mL tube at 4 °C for 20 min. After three brief washes with the binding buffer containing 10 mM imidazole, proteins bound to the resin were eluted with the binding buffer containing 150 mM imidazole. Aliquots of the eluted protein sample (10 μL each) were analyzed by SDS/PAGE and stained with Coomassie brilliant blue. Protein bands specifically bound to the His-tagged bait protein were excised from the gel, and in-gel digestion and peptide mapping of the tryptic digests were performed as described previously (16, 25).

BACTH Assays. Protein–protein interactions in live *E. coli* cells were assayed using the BACTH system based on the reconstitution of adenylate cyclase activity as described previously (28). Briefly, the *cya*-deficient *E. coli* K-12 strain, BTH101, was cotransformed with derivatives of pUT18C and pKT25 encoding T18 and K25 fragments of *B. pertussis* adenylate cyclase, respectively. The cotransformants were spotted on LB plates containing 100 μg/mL streptomycin, 100 μg/mL ampicillin, and 50 μg/mL kanamycin, with 40 μg/mL X-gal as the color indicator for β-galactosidase activity, and then incubated at 30 °C overnight. To quantify the strength of the interaction, the cotransformants were grown in LB medium at 30 °C to stationary growth phase, and the β-galactosidase activity was measured as described by Miller (58).

In Vitro Assay for ppGpp Hydrolase Activity of SpoT. The in vitro ppGpp hydrolase activity of SpoT was assayed in a 30-μL reaction mixture containing 50 mM Tris·HCl (pH 8.0), 4 mM $MnCl_2$, 15 mM Mg-acetate, 10 mM DTT, 90 mM sodium formate, 25 mM ammonium acetate, and indicated concentrations of ppGpp and GST–SpoT protein in the presence of Rsd, HPr or both. After incubation at 37 °C for the indicated time, the reaction was terminated by the addition of 1 μL 88% formic acid, and then trifluoroacetic acid was added to a final concentration of 10%. The reaction product generated from ppGpp was then analyzed by HPLC using a Varian dual pump system connected to an UV-visible detector. A 20-μL reaction mixture was applied to a Supelcosil LC-18-T reverse-phase chromatography column (Sigma Aldrich) equilibrated with 100 mM KH_2PO_4 and 8 mM tetrabutyl ammonium hydrogen sulfate (pH 2.6) in water and then chromatographed using a linear gradient of 0–30% methanol containing 100 mM KH_2PO_4 and 8 mM tetrabutyl ammonium hydrogen sulfate (pH 2.6) at a flow rate of 1 mL/min for 30 min. The eluted nucleotides were detected at 254 nm.

Detection of Intracellular (p)ppGpp Levels. Overnight grown *E. coli* culture was inoculated into fresh low-phosphate (0.2 mM) MOPS minimal medium (59) containing 0.2% galactose and 0.02% arabinose and 100 μCi/mL $^{32}PO_4^{3-}$ to an OD_{600} of 0.05 and incubated with shaking at 37 °C. When OD_{600} reached ∼0.2, serine hydroxamate (1 mg/mL) was added to trigger the stringent response. At the indicated times, 20-μL samples were mixed with an equal volume of 17 M formic acid (30). After four freeze–thaw cycles in liquid nitrogen, the samples were centrifuged at 16,000 × *g* for at least 1 min to remove cell debris. Then 5 μL of supernatants was spotted onto a polyethyleneimine plate (Merck Millipore) and developed in 1.5 M KH_2PO_4 (pH 3.4) as mobile phase at room temperature. The plate was autoradiographed using Bio-imaging Analyzer (FujiFilm) and (p)ppGpp signals were measured using myImageAnalysis Software (Thermo Fisher Scientific).

Determination of the in Vivo Phosphorylation State of HPr. The phosphorylation state of HPr was determined as previously described with some modifications (24). N^1-Phosphohistidine residues are known to be very unstable at neutral and acidic pH, thus exposure of samples to pH < 9.0 was minimized. *E. coli* MG1655/pACYC-HPr was cultivated in LB medium containing the indicated sugars. Cell cultures (0.2 mL at OD_{600} = 0.3) were quenched, the phosphorylation states of HPr were fixed, and the cells were disrupted at the same time by mixing with 15 μL of 5 M NaOH, followed by vortexing for 20 s. After the addition of 45 μL of 3 M sodium acetate (pH 5.2) and 0.65 mL of ethanol, the samples were centrifuged at 16,000 × *g* at 4 °C for 10 min. The pellet was suspended in 20 μL of native PAGE sample buffer containing 1 M urea, and immediately analyzed by 16% native PAGE. Proteins were then electrotransferred onto Immobilon-P (Merck Millipore) following the manufacturer's protocol and HPr was detected by immunoblotting using antiserum against HPr raised in rabbits. The protein bands were visualized using Immobilon Western chemiluminescent HRP substrate (Merck Millipore) following the manufacturer's instructions.

ACKNOWLEDGMENTS. We thank Prof. Chang-Ro Lee at Myongji University for sharing pKT25-EIIA^{Ntr}, pKT25-EIIA^{Ntr}(H73A), and pKT25-EIIA^{Ntr}(H73E) plasmids; and Hyeong-In Ham for critical reading of the manuscript. This work was supported by National Research Foundation Grant NRF-2015R1A2A1A15053739 funded by the Ministry of Science, Information, and Communication Technology. J.-W.L. was supported by the BK21 plus program of the National Research Foundation, Republic of Korea.

1. Cashel M, Gallant J (1969) Two compounds implicated in the function of the RC gene of *Escherichia coli*. *Nature* 221:838–841.
2. Potrykus K, Cashel M (2008) (p)ppGpp: Still magical? *Annu Rev Microbiol* 62:35–51.
3. Haseltine WA, Block R (1973) Synthesis of guanosine tetra- and pentaphosphate requires the presence of a codon-specific, uncharged transfer ribonucleic acid in the acceptor site of ribosomes. *Proc Natl Acad Sci USA* 70:1564–1568.
4. An G, Justesen J, Watson RJ, Friesen JD (1979) Cloning the *spoT* gene of *Escherichia coli:* Identification of the *spoT* gene product. *J Bacteriol* 137:1100–1110.
5. Murray KD, Bremer H (1996) Control of *spoT*-dependent ppGpp synthesis and degradation in *Escherichia coli*. *J Mol Biol* 259:41–57.
6. Brown A, Fernández IS, Gordiyenko Y, Ramakrishnan V (2016) Ribosome-dependent activation of stringent control. *Nature* 534:277–280.
7. Xiao H, et al. (1991) Residual guanosine 3′,5′-bispyrophosphate synthetic activity of *relA* null mutants can be eliminated by *spoT* null mutations. *J Biol Chem* 266: 5980–5990.
8. Vinella D, Albrecht C, Cashel M, D'Ari R (2005) Iron limitation induces SpoT-dependent accumulation of ppGpp in *Escherichia coli*. *Mol Microbiol* 56:958–970.
9. Bougdour A, Gottesman S (2007) ppGpp regulation of RpoS degradation via anti-adaptor protein IraP. *Proc Natl Acad Sci USA* 104:12896–12901.
10. Seyfzadeh M, Keener J, Nomura M (1993) *spoT*-dependent accumulation of guanosine tetraphosphate in response to fatty acid starvation in *Escherichia coli*. *Proc Natl Acad Sci USA* 90:11004–11008.
11. Haugen SP, Ross W, Gourse RL (2008) Advances in bacterial promoter recognition and its control by factors that do not bind DNA. *Nat Rev Microbiol* 6:507–519.
12. Paul BJ, Berkmen MB, Gourse RL (2005) DksA potentiates direct activation of amino acid promoters by ppGpp. *Proc Natl Acad Sci USA* 102:7823–7828.
13. Hauryliuk V, Atkinson GC, Murakami KS, Tenson T, Gerdes K (2015) Recent functional insights into the role of (p)ppGpp in bacterial physiology. *Nat Rev Microbiol* 13: 298–309.
14. Corrigan RM, Bellows LE, Wood A, Gründling A (2016) ppGpp negatively impacts ribosome assembly affecting growth and antimicrobial tolerance in Gram-positive bacteria. *Proc Natl Acad Sci USA* 113:E1710–E1719.
15. Kriel A, et al. (2012) Direct regulation of GTP homeostasis by (p)ppGpp: A critical component of viability and stress resistance. *Mol Cell* 48:231–241.
16. Park YH, Lee CR, Choe M, Seok YJ (2013) HPr antagonizes the anti-σ^{70} activity of Rsd in *Escherichia coli*. *Proc Natl Acad Sci USA* 110:21142–21147.
17. Jishage M, Ishihama A (1998) A stationary phase protein in *Escherichia coli* with binding activity to the major σ subunit of RNA polymerase. *Proc Natl Acad Sci USA* 95: 4953–4958.
18. Barabote RD, Saier MH, Jr (2005) Comparative genomic analyses of the bacterial phosphotransferase system. *Microbiol Mol Biol Rev* 69:608–634.
19. Postma PW, Lengeler JW, Jacobson GR (1993) Phosphoenolpyruvate:carbohydrate phosphotransferase systems of bacteria. *Microbiol Rev* 57:543–594.
20. Deutscher J, Francke C, Postma PW (2006) How phosphotransferase system-related protein phosphorylation regulates carbohydrate metabolism in bacteria. *Microbiol Mol Biol Rev* 70:939–1031.
21. Park YH, Um SH, Song S, Seok YJ, Ha NC (2015) Structural basis for the sequestration of the anti-$\sigma^{(70)}$ factor Rsd from $\sigma^{(70)}$ by the histidine-containing phosphocarrier protein HPr. *Acta Crystallogr D Biol Crystallogr* 71:1998–2008.

22. Piper SE, Mitchell JE, Lee DJ, Busby SJ (2009) A global view of *Escherichia coli* Rsd protein and its interactions. *Mol Biosyst* 5:1943–1947.
23. Schmidt A, et al. (2016) The quantitative and condition-dependent *Escherichia coli* proteome. *Nat Biotechnol* 34:104–110.
24. Choe M, Park YH, Lee CR, Kim YR, Seok YJ (2017) The general PTS component HPr determines the preference for glucose over mannitol. *Sci Rep* 7:43431.
25. Lee CR, Cho SH, Yoon MJ, Peterkofsky A, Seok YJ (2007) *Escherichia coli* enzyme IIA^{Ntr} regulates the K^+ transporter TrkA. *Proc Natl Acad Sci USA* 104:4124–4129.
26. Lee CR, Kim M, Park YH, Kim YR, Seok YJ (2014) RppH-dependent pyrophosphohydrolysis of mRNAs is regulated by direct interaction with DapF in *Escherichia coli*. *Nucleic Acids Res* 42:12746–12757.
27. Hernandez VJ, Bremer H (1991) *Escherichia coli* ppGpp synthetase II activity requires *spoT*. *J Biol Chem* 266:5991–5999.
28. Karimova G, Pidoux J, Ullmann A, Ladant D (1998) A bacterial two-hybrid system based on a reconstituted signal transduction pathway. *Proc Natl Acad Sci USA* 95: 5752–5756.
29. Gentry DR, Cashel M (1996) Mutational analysis of the *Escherichia coli spoT* gene identifies distinct but overlapping regions involved in ppGpp synthesis and degradation. *Mol Microbiol* 19:1373–1384.
30. Mechold U, Murphy H, Brown L, Cashel M (2002) Intramolecular regulation of the opposing (p)ppGpp catalytic activities of Rel(*Seq*), the Rel/Spo enzyme from *Streptococcus equisimilis*. *J Bacteriol* 184:2878–2888.
31. Battesti A, Bouveret E (2006) Acyl Carrier protein/SpoT interaction, the switch linking SpoT-dependent stress response to fatty acid metabolism. *Mol Microbiol* 62: 1048–1063.
32. Atkinson GC, Tenson T, Hauryliuk V (2011) The RelA/SpoT homolog (RSH) superfamily: Distribution and functional evolution of ppGpp synthetases and hydrolases across the tree of life. *PLoS One* 6:e23479.
33. Sankaranarayanan R, et al. (1999) The structure of threonyl-tRNA synthetase-tRNA(Thr) complex enlightens its repressor activity and reveals an essential zinc ion in the active site. *Cell* 97:371–381.
34. Wolf YI, Aravind L, Grishin NV, Koonin EV (1999) Evolution of aminoacyl-tRNA synthetases—Analysis of unique domain architectures and phylogenetic trees reveals a complex history of horizontal gene transfer events. *Genome Res* 9:689–710.
35. Karstens K, Zschiedrich CP, Bowien B, Stülke J, Görke B (2014) Phosphotransferase protein $EIIA^{Ntr}$ interacts with SpoT, a key enzyme of the stringent response, in *Ralstonia eutropha* H16. *Microbiology* 160:711–722.
36. Ronneau S, Petit K, De Bolle X, Hallez R (2016) Phosphotransferase-dependent accumulation of (p)ppGpp in response to glutamine deprivation in *Caulobacter crescentus*. *Nat Commun* 7:11423.
37. Kuroda A, Murphy H, Cashel M, Kornberg A (1997) Guanosine tetra- and pentaphosphate promote accumulation of inorganic polyphosphate in *Escherichia coli*. *J Biol Chem* 272:21240–21243.
38. Dalebroux ZD, Swanson MS (2012) ppGpp: Magic beyond RNA polymerase. *Nat Rev Microbiol* 10:203–212.
39. Mitchell JE, et al. (2007) The *Escherichia coli* regulator of sigma 70 protein, Rsd, can up-regulate some stress-dependent promoters by sequestering sigma 70. *J Bacteriol* 189:3489–3495.
40. Neira JL, et al. (2018) The histidine phosphocarrier protein, HPr, binds to the highly thermostable regulator of sigma D protein, Rsd, and its isolated helical fragments. *Arch Biochem Biophys* 639:26–37.
41. Lazzarini RA, Cashel M, Gallant J (1971) On the regulation of guanosine tetraphosphate levels in stringent and relaxed strains of *Escherichia coli*. *J Biol Chem* 246: 4381–4385.
42. Sun D, et al. (2010) A metazoan ortholog of SpoT hydrolyzes ppGpp and functions in starvation responses. *Nat Struct Mol Biol* 17:1188–1194.
43. Deutscher J, et al. (2014) The bacterial phosphoenolpyruvate:carbohydrate phosphotransferase system: Regulation by protein phosphorylation and phosphorylation-dependent protein-protein interactions. *Microbiol Mol Biol Rev* 78:231–256.
44. Harshman RB, Yamazaki H (1971) Formation of ppGpp in a relaxed and stringent strain of *Escherichia coli* during diauxie lag. *Biochemistry* 10:3980–3982.
45. Traxler MF, Chang DE, Conway T (2006) Guanosine 3′,5′-bispyrophosphate coordinates global gene expression during glucose-lactose diauxie in *Escherichia coli*. *Proc Natl Acad Sci USA* 103:2374–2379.
46. Braedt G, Gallant J (1977) Role of the *rel* gene product in the control of cyclic adenosine 3′,5′-monophosphate accumulation. *J Bacteriol* 129:564–566.
47. Baba T, et al. (2006) Construction of *Escherichia coli* K-12 in-frame, single-gene knockout mutants: The Keio collection. *Mol Syst Biol* 2:2006.0008.
48. Shyp V, et al. (2012) Positive allosteric feedback regulation of the stringent response enzyme RelA by its product. *EMBO Rep* 13:835–839.
49. Raskin DM, Judson N, Mekalanos JJ (2007) Regulation of the stringent response is the essential function of the conserved bacterial G protein CgtA in *Vibrio cholerae*. *Proc Natl Acad Sci USA* 104:4636–4641.
50. Verstraeten N, et al. (2015) Obg and membrane depolarization are part of a microbial bet-hedging strategy that leads to antibiotic tolerance. *Mol Cell* 59:9–21.
51. Persky NS, Ferullo DJ, Cooper DL, Moore HR, Lovett ST (2009) The ObgE/CgtA GTPase influences the stringent response to amino acid starvation in *Escherichia coli*. *Mol Microbiol* 73:253–266.
52. Loveland AB, et al. (2016) Ribosome•RelA structures reveal the mechanism of stringent response activation. *eLife* 5:e17029.
53. Dai X, et al. (2016) Reduction of translating ribosomes enables *Escherichia coli* to maintain elongation rates during slow growth. *Nat Microbiol* 2:16231.
54. Aizenman E, Engelberg-Kulka H, Glaser G (1996) An *Escherichia coli* chromosomal "addiction module" regulated by guanosine [corrected] 3′,5′-bispyrophosphate: A model for programmed bacterial cell death. *Proc Natl Acad Sci USA* 93:6059–6063; erratum in *Proc Natl Acad Sci USA* (1996) 93:9991.
55. Datsenko KA, Wanner BL (2000) One-step inactivation of chromosomal genes in *Escherichia coli* K-12 using PCR products. *Proc Natl Acad Sci USA* 97:6640–6645.
56. Park S, Park YH, Lee CR, Kim YR, Seok YJ (2016) Glucose induces delocalization of a flagellar biosynthesis protein from the flagellated pole. *Mol Microbiol* 101:795–808.
57. Kim HM, Park YH, Yoon CK, Seok YJ (2015) Histidine phosphocarrier protein regulates pyruvate kinase A activity in response to glucose in *Vibrio vulnificus*. *Mol Microbiol* 96:293–305.
58. Miller JH (1972) *Experiments in Molecular Genetics* (Cold Spring Harbor Lab Press, Cold Spring Harbor, NY).
59. Mechold U, Potrykus K, Murphy H, Murakami KS, Cashel M (2013) Differential regulation by ppGpp versus pppGpp in *Escherichia coli*. *Nucleic Acids Res* 41:6175–6189.